INFECTION AND IMMUNITY, July 2005, p. 4025–4033 Vol. 73, No. 7
0019-9567/05/$08.00+0 doi:10.1128/IAI.73.7.4025–4033.2005

Identification of Novel Genes in Intestinal Tissue That Are Regulated after Infection with an Intestinal Nematode Parasite

R. Datta,[1] M. L. deSchoolmeester,[1] C. Hedeler,[2] N. W. Paton,[2] A. M. Brass,[2] and K. J. Else[1]*

Faculty of Life Sciences, University of Manchester, Michael Smith Building, Oxford Road, Manchester M13 9PT, United Kingdom,[1] and Department of Computer Science, University of Manchester, Oxford Road, Manchester M13 9PL, United Kingdom[2]

Received 8 July 2004/Returned for modification 23 August 2004/Accepted 28 February 2005

Infection of resistant or susceptible mice with *Trichuris muris* provokes mesenteric lymph node responses which are polarized towards Th2 or Th1, respectively. These responses are well documented in the literature. In contrast, little is known about the local responses occurring within the infected intestine. Through microarray analyses, we demonstrate that the gene expression profile of infected gut tissue differs according to whether the parasite is expelled or not. Genes differentially regulated postinfection in resistant BALB/c mice include several antimicrobial genes, in particular, intelectin (Itln). In contrast, analyses in AKR mice which ultimately progress to chronic infection provide evidence for a Th1-dominated mucosa with up-regulated expression of genes regulated by gamma interferon. Increases in the expression of genes associated with tryptophan metabolism were also apparent with the coinduction of tryptophanyl tRNA synthetase (Wars) and indoleamine-2,3-dioxygenase (Indo). With the emerging literature on the role of these gene products in the suppression of T-cell responses in vitro and in vivo, their up-regulated expression here may suggest a role for tryptophan metabolism in the parasite survival strategy.

Expulsion of the cecum-dwelling nematode parasite *Trichuris muris* is dependent on the strain of mouse infected and correlates precisely with the type of T-helper cell provoked. Resistance requires a dominant Th2 response; susceptible mice mount a strong but inappropriate Th1 response (13). There is considerable and detailed literature demonstrating the immune polarization of the mesenteric lymph node cell response towards Th2 in resistant mice (e.g., BALB/c) and Th1 in susceptible mice (e.g., AKR) (4, 9, 13, 17, 20, 23). In order to effect worm expulsion, Th2 cells are then recruited to the site of infection, where they mediate worm expulsion by some as-yet-undefined Th2-controlled effector mechanism (7). The intracellular niche within intestinal epithelial cells occupied by *T. muris* presents an intimate association between parasite and host. Postinfection morphological changes in the gut architecture occur with epithelial cell hyperproliferation and crypt cell hyperplasia (3). Surprisingly, the cellular infiltrate which develops postinfection has not been characterized in any great detail, although infection does provoke a mild mastocytosis and eosinophilia and the recruitment of $CD4^+$ T cells and macrophages (2). Schopf et al. (41) analyzed the levels of cytokine mRNA in cecal tissue from *T. muris*-infected C57BL/6 mice and a variety of cytokine knockout mice by reverse transcription (RT)-PCR. Their results showed an elevation in the transcripts for gamma interferon (IFN-γ) in gut tissue from susceptible mice. Beyond those studies (2, 41), there is a general lack of knowledge surrounding the events which occur locally in the large intestinal tissue and the mechanisms which prelude either worm expulsion or worm persistence. This prompted us to analyze the broad gene expression profiles of mucosal tissue from resistant and susceptible mice. We chose two time points: day 19, a time point when worm experience is similar but outcome of infection is disparate, with BALB/c mice having recently resolved infection while worms persist in AKR mice, and day 60, a time point well into chronic infection in AKR mice but 40 days beyond the BALB/c host's recent experience of worms. mRNA from AKR and BALB/c gut tissue was analyzed by microarray, and key changes in gene expression were confirmed by semiquantitative RT-PCR or protein analyses where possible. Data generated present a picture at the level of the transcriptome of two very different local gut environments in resistant and susceptible mice at day 19 postinfection, dominated by antimicrobial factors and by IFN-γ-induced genes, respectively. The epithelial cell was identified as a cellular source of two of the most differentially expressed genes. Further, analyses at day 60 demonstrate that the chronically infected gut remains a highly active environment in terms of gene expression, while the resistant gut resolves back to a resting state.

MATERIALS AND METHODS

Animals. Male AKR and BALB/c mice (Harlan UK) were infected at 6 to 8 weeks of age and killed at various time points postinfection, as described in the text, in group sizes of five mice unless otherwise indicated. All experiments were performed under the regulations of the Home Office Scientific Procedures Act (1986).

Parasite. Mice were infected with 200 embryonated eggs by oral gavage. Worm burdens were assessed at days 19 and 60 as previously described (14).

Isolation of intestinal epithelial cells. All tissue culture media were purchased from Invitrogen (Paisley, United Kingdom), and other chemicals were purchased from Sigma (Poole, United Kingdom). The large intestine (cecum and approximately 5 cm of colon) was recovered, and fat, connective tissue, and cecal patch lymphoid follicles were removed. The tissue was then slit longitudinally and rinsed in calcium- and magnesium-free Hanks balanced salt solution containing 2% fetal calf serum (FCS) (CMF2%), cut into 1-cm pieces, and placed into ice-cold CMF2%. Following vigorous shaking, the supernatant was discarded

* Corresponding author. Mailing address: Faculty of Life Sciences, University of Manchester, Michael Smith Building, Oxford Road, Manchester M13 9PT, United Kingdom. Phone: 44 (0) 161-275-5213. Fax: 44 (0) 161-275-5656. E-mail: kathryn.j.else@manchester.ac.uk.

and fresh CMF2% was added. This was repeated until the supernatant was clear. The tissue was then placed into calcium- and magnesium-free Hanks balanced salt solution containing 10% FCS, 1 mM EDTA, 1 mM dithiothreitol, 100 units/ml penicillin, and 100 μg/ml streptomycin (CMF10%) and incubated at 37°C for 20 min. After vigorous shaking, the supernatant was recovered and placed on ice. This procedure was repeated once more. The supernatant was then passed through a 100-μm cell strainer (Becton Dickinson, Oxford, United Kingdom) and centrifuged at 200 × *g* for 10 min. The cells were resuspended in ice-cold RPMI medium containing 10% FCS, 2 mM L-glutamine, 100 units/ml penicillin, 100 μg/ml streptomycin, and 60 μM monothioglycerol and counted, and the volume was adjusted to give 5×10^6 cells/ml. Aliquots were taken for flow cytometric analysis and total RNA extraction.

Flow cytometry. Cells were stained with rat anti-mouse Ep-CAM (clone G8.8) which binds to a mouse epithelial cell marker and was kindly donated by G. Anderson. The percentage of cells binding G8.8 was determined by a secondary antibody, anti-rat immunoglobulin G2a (IgG2a)-fluorescein isothiocyanate (Serotec, Oxford, United Kingdom). Isotype controls were performed using rat IgG2a of irrelevant specificity (anti-keyhole limpet hemocyanin; BD Biosciences, Oxford, United Kingdom) and the same secondary antibody, anti-rat IgG2a-fluorescein isothiocyanate. Leukocyte contamination of intestinal epithelial cell preparations was assessed by the use of rat anti-mouse CD45-phycoerythrin (Serotec) (isotype control, rat IgG2b-phycoerythrin; Caltag, Towcester, United Kingdom). Cells were stained for 30 min on ice in the dark before being fixed with 1% paraformaldehyde in phosphate-buffered saline and stored at 4°C in the dark until analyzed. Results were acquired with a FACSCaliber flow cytometer and analyzed using CellQuest Pro software (both from BD Biosciences). At all time points, ≥90% of cells were positive for G8.8, whereas ≤1% were positive for CD45.

Serum parasite-specific antibody enzyme-linked immunosorbent assay (ELISA). Ninety-six-well plates (Dynex, Billingshurst, West Sussex, United Kingdom) were coated with 5 μg/ml *T. muris* excretory/secretory antigen in carbonate buffer, pH 9.6, at 50 μl/well. Sera were serially diluted in phosphate-buffered saline containing 0.05% Tween 20 from 1:20 to 1:2,560. Antigen-specific antibodies were detected using biotinylated rat anti-IgG1 (Serotec Ltd., Oxford, United Kingdom) or rat anti-IgG2a (Pharmingen) followed by streptavidin-conjugated horseradish peroxidase (Boehringer Mannheim, Germany). 2,2-Azino-bis-(3-ethylbenz-thiazoline-6-sulfonic acid) (Sigma) at 1 mg/ml in citrate buffer with 0.003% H_2O_2 was used as a substrate, and plates were read at 405 nm with a 490-nm reference filter.

Serum MMCP-1. Mouse mast cell protease 1 (MMCP-1) was detected in sera using a commercially available ELISA kit form Moredun Scientific (Penucuik, Scotland). Briefly, ELISA plates were coated overnight at 4°C with 50 μl sheep anti-MMCP-1 capture antibody at 2 μg/ml. Serial dilutions of MMCP-1 standard or samples were applied followed by a rabbit anti-MMCP-1 horseradish peroxidase conjugate at a 1/1,000 dilution. The substrate 2,2-azino-bis-(3-ethylbenz-thiazoline-6-sulfonic acid) (Sigma) at 1 mg/ml in citrate buffer with 0.003% H_2O_2 was added, and plates were read at 405 nm with a 490-nm reference filter.

RNA isolation and cDNA synthesis. One centimeter of colonic tissue immediately adjacent to the cecum was homogenized in TRIZol (Invitrogen), and RNA was isolated according to the manufacturer's instructions. RNA samples were treated with DNase (Ambion) to remove traces of contaminating DNA. The concentration of RNA was estimated using a spectrophotometer at a 260-nm wavelength (Phamacia Biotech), and the quality was assessed by gel electrophoresis. First-strand cDNA synthesis was performed using oligo$(dT)_{15}$ as a primer and Im Prom II RT enzyme (Promega, United Kingdom) following the protocol standardized by the Human Genome Mapping Project Resource Centre, Harwell, United Kingdom (http://www.hgmp.mrc.ac.uk). cDNA mix was treated with RNase (Sigma) to eliminate traces of RNA and was purified using Amicon Mirocon-PCR filters (Millipore). The quantity of cDNA was estimated by a spectrophotometer at 260 nm, and the quality was assessed by visualizing on 1% agarose gel. cDNA from five mice per group was pooled, and 2.5 μg of the pooled purified target cDNA was labeled with the fluorescent dyes Cye5-dCTP and Cye3-dCTP (Amersham Biosciences, United Kingdom) using a Bioprime labeling kit (Invitrogen, United Kingdom). Labeled cDNAs were purified using Probequant Sephadex G50 columns (Amersham Biosciences, United Kingdom) to remove unincorporated nucleotides and were pooled together within a group. Poly(dA) (5.0 μl; Amersham Biosciences, United Kingdom) and mouse cot DNA (10.0 μl; Invitrogen, United Kingdom) were added to the pooled DNA mix to block nonspecific targets. The resulting mix was concentrated to 10 to 15 μl using a vacuum centrifuge and diluted with 10.0 μl of sterile water and 25.0 μl of hybridization solution to make the volume 40 to 45 μl. Prior to use, the mix was heated at 85°C for 5 min and then incubated at 42°C for 30 to 60 min.

Oligonucleotide microarrays. The mouse "known" gene SGC oligonucleotide set microarrays were obtained from the Medical Research Council Rosalind Franklin Centre for Genomics Research (formally the Human Genome Mapping Project Resource Centre) and consisted of ~9,000 genes spotted in duplicate on glass slides. Analyses of data generated revealed this particular type of array to be robust and accurate for high-intensity spots. However, these analyses also revealed a loss of sensitivity for low-abundance transcripts (with an increase in error measured from technical repeats with decreasing intensity). Microarray slides were hybridized with fluorescently labeled cDNA targets, prepared as described above, scanned using a GenePix 4000A Axon scanner, and analyzed using GenePix Pro 4 and Max D analysis software (http://www.bioinf.man.ac.uk/microarray/maxd/) and GIMS (8). Each hybridization compared gene expression levels in infected tissue to those in uninfected tissue of that mouse strain, gut tissue was pooled from five individual animals, and two independent infection experiments were run. The average $\log_2$-fold changes (infected tissue over uninfected tissue) presented represent values calculated from both infection experiments. Hybridizations included reverse labeling experiments where the fluorescent dyes were incorporated into the alternative cDNA target.

Normalization. The array normalization was based on recent work (16) that used a simple statistical model to explore the error inherent in using log ratios from fluor-reversed microarrays and which then optimized the normalization to minimize that error. We start by defining the measured log ratio (M) and log spot intensity (A) as follows: $M = \log R/G$ and $A = \log[\sqrt{(RG)}]$, where R and G are measurements from the red and green channels, respectively (logarithms are to base 2). Let n represent the number of replicates of an experiment, g represent the number of the features (probes) on the slide, m_j ($j = 1, 2, \ldots, g$) represent the true ratio of expression levels for the gene measured by feature j, and M_{jk} ($j = 1, 2, \ldots, g$; $k = 1, 2, \ldots, n$) represent the measured ratio of expression levels for feature j on replicate k.

The measurement M_{jk} can be modeled as follows: $M_{jk} = m_j + c + c_k + e(F_j) + e_k(A_{jk}) + e_k(P_j) + \epsilon_{jk}$, where c represents the expected global measurement bias between two channels, c_k represents the variation of global measurement bias shown on replicate k, $e(F_j)$ represents feature-specific bias for feature j, $e_k(A_{jk})$ represents spot intensity-dependent bias for feature j on replicate k, $e_k(P_j)$ represents spot location-related bias for feature j on replicate k, and ϵ_{jk} represents the zero mean random error introduced to feature j on replicate k. By a suitable choice of normalization strategies, it is possible to minimize $e(F_j)$, $e_k(A_{jk})$, and $e_k(P_j)$ and therefore to estimate ϵ_{jk}.

We can therefore create an error matrix ϵ, where the (j,k)th element is the random error in spot j from the dye flip pair of chips k, ϵ_{jk}. The average value of $(\epsilon_{jk})^2$ down a column, E_k, provides an estimate of the chip error. Chips with a value for E_k that is significantly different from the value across all chips are regarded as suspect. E_k therefore provides a useful quality metric for chip quality control and for eliminating poor-quality chip pairs from further analysis (unpublished data). The average value of $(\epsilon_{jk})^2$ along a row, E_j, provides an estimate of error in the spot reading, i.e., the random error expected from technical repeats. In the experiments presented here, the root mean squared value of this error was about 0.1, suggesting that the log ratios being measured on the chip were on average accurate, ±0.1. This value is smaller than the typical variation seen in log ratio values between the biological repeats.

Semiquantitative RT-PCR. Gut cDNAs used in the microarray hybridizations were also used for corroborative semiquantitative RT-PCR. Twofold serial dilutions were made in a 25-μl reaction volume with *Taq* DNA polymerase (Promega, Southampton, United Kingdom) for hypoxanthine phosphoribosyltransferase (HPRT) (5′-GTAATGATCAGTCAACGGGGGAC-3′ and 5′-CCAGCAAGCTTGCAACCTTAACCA-3′), indoleamine-2,3-dioxygenase (Indo) (5′-CTGCACGACATAGCTACCAGTCTG-3′ and 5′-ACATTTGAGGGCTCTTCCGACTTG-3′), intelectin (Itln) (5′-GAAGGTAACCCCGTGCAGTGTG-3′ and 5′-GGAGCCCACAATGGAGAAGTCAG-3′), CXCL9 (Mig) (5′-CTTCTGAGGCTCACGTCACCAAG-3′ and 5′-ATCCCATGGTCTCGAAAGCTACG-3′), and CXCL11 (I-Tac) (5′-GTCTGACTGTGAGCCCTCCA-3′ and 5′-GTGCCTCGTGATATTTGGGGAA-3′). The starting amounts of cDNA for indoleamine-2,3-dioxygenase, intelectin, CXCL9, and CXCL11 were determined by PCR for HPRT. Thus, cDNAs for HPRT were titrated out, and nonsaturated dilutions giving bands of equivalent brightness were selected. RT-PCR analysis of gamma interferon was done on individual and pooled gut cDNAs using the primers 5′-AGCTCTTCCTCATGGCTGTTTC-3′ and 5′-ATGTTGTTGCTGATGGCCTGA-3′. PCR cycle numbers were 30 cycles for indoleamine-2,3-dioxygenase, 33 cycles for intelectin, 34 cycles for CXCL9, 32 cycles for CXCL11, and 35 cycles for gamma interferon. The expression level of each transcript was evaluated after ethidium bromide staining on 2% agarose gel.

Total RNA was extracted from 5×10^6 freshly isolated intestinal epithelial cells using TRIzol (Invitrogen) according to the manufacturer's instructions.

RNA was assessed by spectrometry and gel electrophoresis and stored at −80°C. Oligo(dT)$_{18}$-primed cDNA was synthesized from 0.5 μg of RNA using Superscript II reverse transcriptase (Invitrogen). Twofold serial dilutions were analyzed by PCR in 25-μl reaction volumes with *Taq* DNA polymerase (Promega, Southampton, United Kingdom) for HPRT, indoleamine-2,3-dioxygenase, and intelectin primers as described above. The starting amounts of cDNA for indoleamine-2,3-dioxygenase and intelectin were determined by PCR for HPRT. Thus, cDNAs for HPRT were titrated out, and nonsaturated dilutions giving bands of equivalent brightness were selected. The number of PCR cycles was 28 for HPRT, 30 for indoleamine-2,3-dioxygenase, and 32 for intelectin.

Statistical analyses. Significance analysis of microarrays (SAM) (44) was used to analyze the data from the AKR and BALB/c mice at day 19 and day 60. It was observed that genes with a $\log_2$ ratio ≥0.9 had q values of 2.5%. (two-class unpaired data, 100 permutations; delta = 0.55). In all experiments, we therefore used a $\log_2$ ratio cutoff of 0.9 for genes to include for further analysis. Significant differences ($P < 0.05$) in MMCP-1 levels were determined using analysis of variance with Bonferroni's multiple comparison test.

RESULTS

Adult worms chronically infected the AKR mouse strain to at least day 60 postinfection (one of two experiments [data not shown]). Although some resolution of worm burden was evident from the levels at day 19, all mice harbored fecund adult worms at a time point over 3 weeks beyond the time point previously used to define chronic infection (day 35). Microarray analyses at day 60 postinfection thus allow insights at the level of the transcriptome into the mechanisms of persisting chronic infection in the AKR mouse. In contrast, mice of the BALB/c strain expelled the parasite by day 19 (worm counts 0, 0, 1, 0, and 0 [one of two experiments]), providing a time point postinfection when the transcriptional responses within the gut are associated with worm expulsion. Analyses of the parasite-specific IgG1 and IgG2a antibody responses at day 60 postinfection revealed a strong IgG1 response in both resistant and susceptible mouse strains but an IgG2a response associated uniquely with worm persistence (one of two experiments [data not shown]). The same profile was seen at day 19, although optical densities were lower (data not shown). These data thus conform to the results of previous publications (4, 13) reporting serological analyses up to day 35 postinfection and linking these IgG isotype profiles to a dominant Th1 response in susceptible mice and a dominant Th2 response in resistant mice.

Transcriptional responses of infected gut tissue. Microarray analyses were performed on gut tissue taken at day 19 and day 60 postinfection from AKR and BALB/c mice. Each hybridization compared gene expression levels in infected tissue to those of uninfected tissue of the same mouse strain, gut tissue was pooled from five individual animals, and two independent infection experiments were performed. The $\log_2$-fold changes presented represent average values calculated from both infection experiments. In some cases, individual gut tissues were also analyzed to confirm the robustness of the gene expression data.

Figure 1 shows a scatter plot representing the average $\log_2$-fold changes for genes with up-regulated or down-regulated expression postinfection in AKR and BALB/c mice at day 19 postinfection. Genes regulated by an average $\log_2$-fold change of ≥0.9 or ≤−0.9 have a false discovery rate of 2.9% by SAM analysis (44), and thus, these thresholds are used to identify genes with increased or decreased expression. Quantitatively, the gene expression profile of gut tissue from a susceptible mouse was very different from that of a resistant mouse. Thus, AKR mice up-regulated (average $\log_2$-fold change of ≥0.9) the expression of 12 known genes and down-regulated (average $\log_2$-fold change of ≤−0.9) 33 genes. In the BALB/c host, only 7 known genes were up-regulated and 11 were down-regulated. Surprisingly, of the known genes which showed altered levels of expression (up or down), only six genes were common to both mouse strains, including mouse mast cell protease 1 (*Mcpt1* [up-regulated in both strains]). Qualitatively, the genes which were regulated postinfection in the AKR mouse were very different from those regulated in the BALB/c host. Interestingly, transcripts for a number of IFN-γ-regulated genes, including indoleamine-2,3-dioxygenase (Indo), tryptophan-tRNA synthetase (Wars), the chemokines CXCL9 (Cxcl9) and CXCL11 (Cxcl11), T-cell-specific GTPase (Tgtp), and alpha interferon-inducible protein (G1p2), were elevated in AKR, but not BALB/c, mice. AKR mice also had increased levels of transcripts for Ia-associated invariant chain (Ii), Z-DNA binding protein 1 (Zbp1), coagulation factor VIII (F8), and keratin-associated protein 5-4 (Krtap5-4). Gene expression of pancreatitis-associated protein (Pap) was up-regulated in AKR mice and down-regulated in BALB/c mice in the context of infection. However, when hybridizations using naïve gut tissue

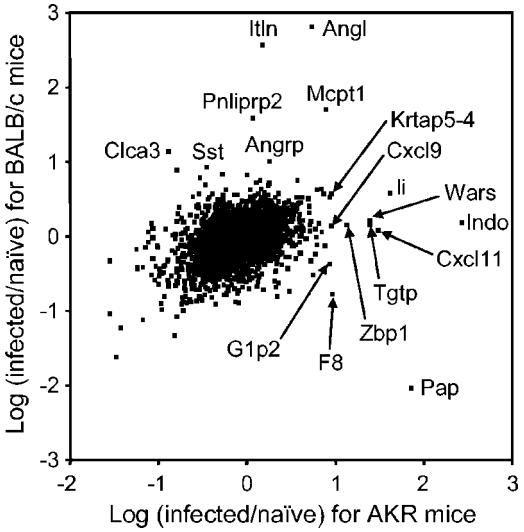

FIG. 1. Transcriptome analyses of *Trichuris*-infected gut tissue from resistant and susceptible mice at day 19 postinfection. The scatter plot shows the average $\log_2$-fold changes in gene expression in gut tissue from AKR mice at day 19 compared to that from uninfected mice (x axis) versus the average $\log_2$-fold changes in gene expression in gut tissue from BALB/c mice at day 19 compared to that from uninfected mice (y axis). Genes up-regulated in AKR and/or BALB/c gut tissue are labeled by gene symbol: indoleamine-2,3-dioxygenase (Indo), pancreatitis-associated protein (Pap), Ia-associated invariant chain (Ii), CXCL11 (Cxcl11), tryptophan tRNA synthase (Wars), T-cell-specific GTPase (Tgtp), Z-DNA binding protein 1 (Zbp1), CXCL9 (Cxcl9), coagulation factor VIII (F8), keratin-associated protein 5-4 (Krtap5-4), interferon alpha-inducible protein (G1p2), mouse mast cell protease 1 (Mcpt1), angiogenin like (Angl), intelectin (Itln), pancreatic lipase-related protein 2 (Pnliprp2), chloride channel calcium-activated 3 (Clca3), angiogenin-related protein (Angrp), and somatostatin (Sst). Genes regulated by an average $\log_2$-fold change of ≥+0.9 or ≤−0.9 have a false discovery rate at this threshold of 2.9% by SAM analysis (44). Gut tissue was pooled from five individual animals within a group, and two independent infection experiments were run. The average $\log_2$-fold changes presented represent values calculated from both infection experiments.

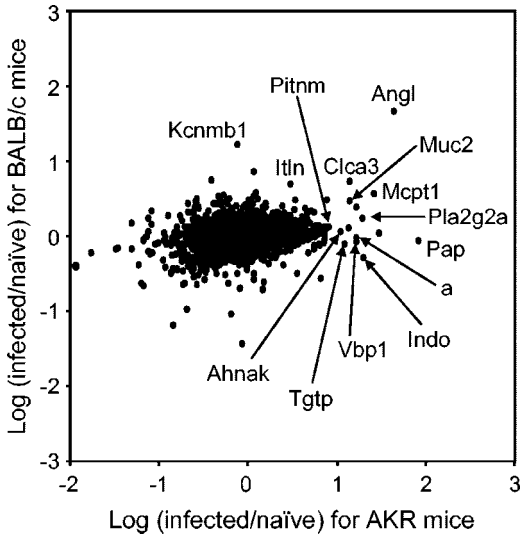

FIG. 2. Altered levels of gene expression are still evident in chronically infected mice but not resistant mice at day 60 postinfection. The scatter plot shows the average $\log_2$-fold changes in gene expression in gut tissue from AKR mice at day 60 compared to that from uninfected mice (*x* axis) versus the average $\log_2$-fold changes in gene expression in gut tissue from BALB/c mice at day 60 compared to that from uninfected mice (*y* axis). Genes up-regulated in AKR and/or BALB/c gut tissue are labeled by gene symbol: angiogenin-like (Angl), pancreatitis-associated protein (Pap), mouse mast cell protease 1 (Mcpt1), indoleamine-2,3-dioxygenase (Indo), phospholipase A2 group IIA (Pla2g2a), mucin 2 (Muc2), von Hippel-Lindau binding protein 1 (Vbp1), nonagouti (a), chloride channel calcium-activated 3 (Clca3), T-cell-specific GTPase (Tgtp), desmoyokin (Ahnak), K-large-conductance calcium (Kcnmb1), and phosphatidylinositol membrane associated (Pitnm). Genes regulated by an average $\log_2$-fold change of $\geq +0.9$ or ≤ -0.9 have a false discovery rate at this threshold of 2.9% by SAM analysis (44). Gut tissue was pooled from five individual animals within a group, and two independent infection experiments were run. The average $\log_2$-fold changes presented represent values calculated from both infection experiments.

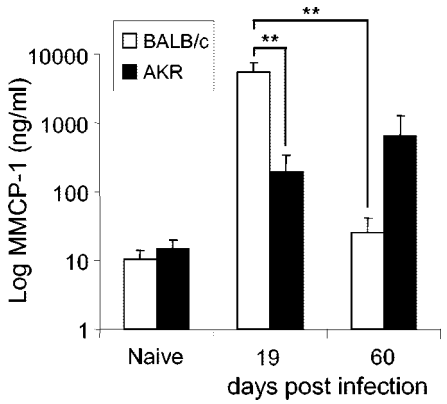

FIG. 3. Serum mast cell protease 1 protein levels precisely mirror changes in mRNA levels revealed by microarray. MMCP-1 levels in the sera of infected AKR and BALB/c mice at day 19 and day 60 postinfection compared to uninfected (naïve) levels are shown. Significantly higher levels of MMCP-1 were seen in BALB/c mice at day 19 postinfection ($^{**}P < 0.001$) than in AKR mice at this time point, with levels declining by day 60 postinfection. Levels of MMCP-1 in AKR mice show a gradual rise postinfection. Levels are means ± standard deviations for five mice per time point.

from the two mouse strains were conducted to address strain-specific differences in gene expression irrespective of infection, Pap showed a strain-specific difference, with uninfected BALB/c mice having much lower levels of expression of this gene than uninfected AKR mice (data not shown). None of the other genes represented in Fig. 1 were significantly different between the two uninfected mouse strains. Relatively more genes were down-regulated in infected AKR gut tissue than up-regulated, and these included the transcript for carbonic anhydrase 2 (average $\log_2$-fold change, −1.0).

The gene expression profile of gut tissue from resistant BALB/c mice was quite distinct from that of susceptible AKR mice (Fig. 1). Here, the expression levels of the antimicrobial factors intelectin (Itln), angiogenin-like protein (Angl), and angiogenin-related protein (Angrp), plus other genes including chloride channel calcium-activated 3 (Clca3) and pancreatic lipase-related protein 2 (Pnliprp2), were up-regulated. These genes were not significantly up-regulated in the AKR mouse (Fig. 1).

The expression levels of genes in gut tissue of AKR and BALB/c mice at day 60 postinfection are depicted by a scatter plot in Fig. 2. In AKR mice which still harbor parasites, Indo and Tgtp remain elevated. In addition, the expression levels of other genes have increased, including ones seen only in the BALB/c mice at day 19 (Angl and Clca3) (Fig. 1). Mcpt1 expression levels at day 60 are higher than at day 19 in the AKR mouse, although not as high as those seen in BALB/c mice at day 19. Transcripts for other genes not apparent at day 19 are also elevated, including mucin 2 (Muc2), Von Hippel-Lindau binding protein 1 (Vbp1), and desmoyokin (Ahnak). Down-regulated genes include carbonic anhydrase 2 (average $\log_2$-fold change, −1.1) and aquaporin 8 (average $\log_2$-fold change, −1.1). In the absence of an infection for over 40 days, the BALB/c gut tissue is largely unchanged from naïve expression levels, represented by dots clustering around the 0 value of the *y* axis (Fig. 2), although Angl remains elevated above a $\log_2$ 0.9-fold change and transcripts for a potassium channel are raised (Kcnmb1, K large conductance-calcium). Quantitatively, the transcripts for 12 known genes are up-regulated (average $\log_2$-fold change of ≥ 0.9), and 28 are down-regulated (average $\log_2$-fold change, ≤ -0.9) in the AKR gut tissue a day 60, compared to just 2 up-regulated and 4 down-regulated in gut tissue from BALB/c mice and with just one gene (Angl) common to both mouse strains.

Protein levels of mouse mast cell protease 1 mirror the changes in gene expression determined by microarray. To substantiate the microarray data, five genes were chosen, Mcpt1 (expressed by both infected AKR and BALB/c mice) indoleamine-2,3-dioxygenase, CXCL9 and CXCL11 (expressed by infected AKR mice), and intelectin (expressed by infected BALB/c mice). Protein levels of MMCP-1 were analyzed in the sera of AKR and BALB/c mice on day 19 and day 60 postinfection. Serum MMCP-1 levels are known to correlate well with an ongoing intestinal mastocytosis (2, 27, 29). Although the intestinal mast cell response is not an essential component of the anti-*T. muris* effector mechanism (6), the MMCP-1 analysis does provide a useful way to corroborate the gene expression data at the level of a protein. The results are shown in Fig. 3 and mirror those shown at the mRNA level by microarray

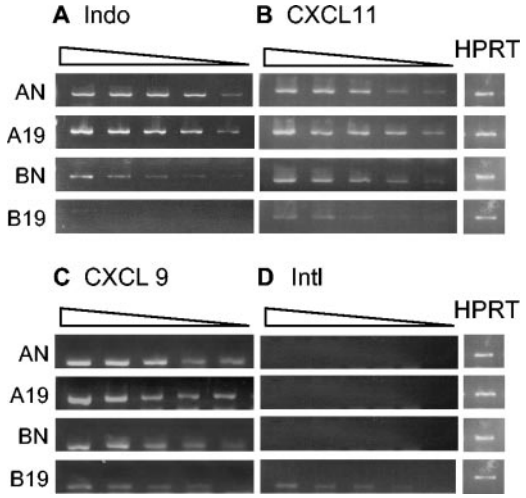

FIG. 4. Semiquantitative RT-PCR confirms the mRNA expression profiles of indoleamine-1,2-dioxygenase, intelectin, CXCL9, and CXCL11 as revealed by microarray. RT-PCR analyses of the expression levels of (A) indoleamine-1,2-dioxygenase (Indo), (B) CXCL11, (C) CXCL9, and (D) intelectin (Itln) at day 19 postinfection in gut tissue from AKR and BALB/c mice are shown. cDNA for HPRT was titrated out, and nonsaturated dilutions giving bands of equivalent brightness, shown as a single band per sample in the figure, were selected as the starting dilution for the serial dilutions. cDNA was serially diluted (1:2) and amplified by PCR as described in Materials and Methods. A, AKR; B, BALB/c. N, naïve; 19, day 19 postinfection.

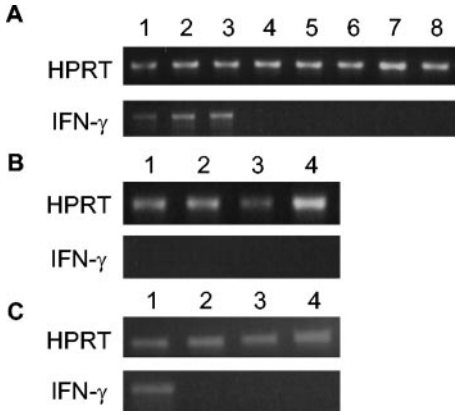

FIG. 5. RT-PCR detects an up-regulation in gamma interferon transcripts postinfection that is not detected by microarray. (A and B) Gamma interferon expression in whole gut tissue from (A) individual infected AKR mice at day 19 postinfection (lanes 1 to 3) and naïve AKR mice (lanes 4 to 8) and (B) infected BALB/c mice (lanes 1 to 2) and naïve BALB/c mice (lanes 3 to 4). (C) Gamma interferon expression in whole gut tissue using the same pools of tissue from infected and naïve AKR and BALB/c mice as those used for microarray analysis. Lane 1, infected AKR; lane 2, naïve AKR; lane 3, infected BALB/c; lane 4, naïve BALB/c. The starting amount of cDNA was determined by PCR for HPRT.

(Fig. 1 and 2). Thus, both mouse strains up-regulate MMCP-1 postinfection when measured by ELISA, with significantly higher levels ($P < 0.001$) in the BALB/c mouse at day 19 compared to levels in AKR mice. By day 60 postinfection, MMCP-1 levels were still rising in the AKR mouse strain, although they had not reached the levels seen in BALB/c mice at day 19. In contrast, levels of this mast cell protease were returning to normal in BALB/c mice. Correlating with this, in BALB/c mice, the average $\log_2$-fold change in gene expression from naïve levels at day 19 was 1.7 (Fig. 1), falling to below 0.9 at day 60 (Fig. 2). In AKR mice, the $\log_2$-fold change in gene expression from naïve levels at day 19 was 0.9 (Fig. 1), rising to 1.4 at day 60 (Fig. 2). Thus, for this particular gene, protein levels determined by ELISA precisely mirror the pattern of change in gene expression determined by microarray.

Gene expression profiles of indoleamine-2,3-dioxygenase, CXCL9, CXCL11, and intelectin are supported by semiquantitative RT-PCR. Using the same cDNAs used for the microarray analyses, semiquantitative RT-PCR was carried out for naïve pooled gut tissue and infected pooled gut tissue from five mice for each strain. The results are shown in Fig. 4 (day 19 postinfection) for the pooled gut tissue samples from both strains. cDNA for each sample was titrated from 1:2 to 1:32. As can be seen in Fig. 4A, uninfected gut tissue from AKR and BALB/c mice expressed indoleamine-2,3-dioxygenase, although expression levels are higher in uninfected AKR mice with transcripts clearly detectable at the 1:32 dilution. However, upon infection, it is only AKR mice which show up-regulated expression of this gene. Similarly, CXCL11 (Fig. 4B) shows an increased level of expression postinfection in AKR mice compared to those of uninfected mice, with brighter bands clearly detected in infected mice at the lower dilutions (1:16 and 1:32). In contrast, the BALB/c host did not up-regulate expression of CXCL11 postinfection. Although the increase in expression postinfection in AKR mice of CXCL9 (Fig. 4C) is less obvious than that for indoleamine-2,3-dioxygenase and CXCL11, it is clear that the BALB/c mouse does not up-regulate expression of this gene postinfection. Thus, the RT-PCR analyses corroborated the up-regulated expression of genes in the AKR mouse. The analyses, however, also revealed an apparent down-regulation in expression of indoleamine-2,3-dioxygenase, CXCL11, and CXCL9 postinfection in BALB/c mice. Using an average $\log_2$-fold change threshold of ≤ -0.9, the expression levels of these genes were not significantly altered by microarray analyses. The results from RT-PCR study do not, however, contradict the microarray data. Rather, they suggest that the differences in gene expression levels in the susceptible mouse upon infection compared to those of the resistant host upon infection are even more pronounced than what was revealed by microarray. Thus, resistant mice actually down-regulate the expression of genes which appeared unchanged by microarray but which susceptible mice clearly up-regulate, as determined by microarray and RT-PCR. RT-PCR analyses of intelectin mRNA confirmed the large differences observed in expression levels of this gene in susceptible AKR and resistant BALB/c mice in response to infection (Fig. 4D). Thus, no transcripts for intelectin were detected in uninfected mice of either strain or in infected AKR mice at day 19. In contrast, a small but clear up-regulation in gene expression was seen in BALB/c mice at this time point.

Although it is not clear why the microarray analyses failed to reveal a significant down-regulation of indoleamine-2,3-dioxygenase, CXCL11, and CXCL9 in infected BALB/c mice compared that to uninfected animals, it may reflect a lack of sensitivity of the microarray technique in detecting significant

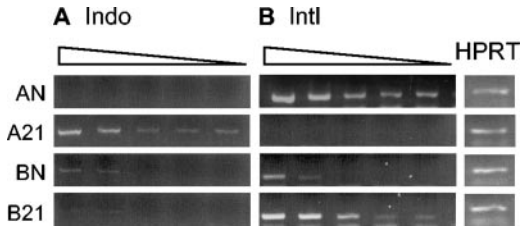

FIG. 6. Epithelial cells are a source of indoleamine-2,3-dioxygenase in susceptible mice and intelectin in resistant mice. Indoleamine-2,3-dioxygenase (A) and intelectin (B) expression in intestinal epithelial cells was measured by RT-PCR. Epithelial cells were isolated from the large intestine of naïve or *T. muris*-infected AKR and BALB/c mice, and total RNA was extracted. cDNA for HPRT was titrated out, and nonsaturated dilutions giving bands of equivalent brightness, shown as a single band per sample in the figure, were selected as the starting dilution for the serial dilutions. cDNA was serially diluted (1:2) and amplified by PCR as described in Materials and Methods. A, AKR; B, BALB/c. N, naïve; 21, day 21 postinfection.

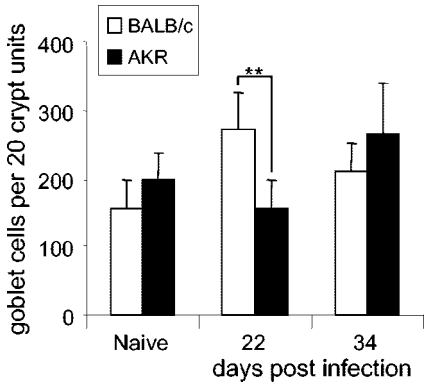

FIG. 7. Goblet cell hyperplasia correlates with worm expulsion in resistant mice. Goblet cell hyperplasia in AKR and BALB/c mice at day 22 and day 34 postinfection were compared to uninfected (naïve) levels. Values are means ± standard deviations for mice per time point from an experiment run separately from the microarray analyses. Goblet cell numbers are significantly elevated ($*P < 0.05$) in BALB/c mice at day 22 postinfection compared to those of AKR mice, a time when transcripts for three antimicrobial proteins (intelectin, angiogenin-like protein, and angiogenin-related protein) show large severalfold increases in this mouse strain.

changes in genes of low abundance. Certainly, for this particular glass oligonucleotide array, we observed a loss in sensitivity for low-abundance transcripts. The relative sensitivity of microarray compared to that of RT-PCR is addressed in Fig. 5A, B, and C. Transcripts for gamma interferon are clearly detectable in the gut tissue of individual infected AKR mice at day 19 postinfection (5A, lanes 1 to 3) compared to those of uninfected animals (Fig. 5B, lanes 4 to 8) and BALB/c mice (Fig. 5B, lanes 1 and 2, infected BALB/c mice, lanes 3 and 4 uninfected BALB/c mice). Transcripts were also detected in the pool of infected gut tissue used directly for the microarray analyses (5C, lane 1). However by microarray, the $\log_2$-fold change at day 19 postinfection for interferon gamma in AKR mice was less than 0.9, at only 0.22.

Intestinal epithelial cells express indoleamine-2,3-dioxygenase and intelectin. To begin to dissect out the cellular sources of the differentially expressed genes, we carried out semiquantitative RT-PCR for indoleamine-2,3-dioxygenase and intelectin on epithelial cells stripped from the intestine of infected mice (day 21 postinfection) and naïve mice (routinely, 90% were G8.8 positive and <1% were CD45 positive). These studies were performed on groups of mice separate from those used in the microarray experiments. The results are shown in Fig. 6. Expression levels of indoleamine-2,3-dioxygenase are up-regulated from naïve levels in epithelial cells from AKR mice postinfection but not in epithelial cells from BALB/c mice postinfection. In contrast, transcripts for intelectin are up-regulated from naïve levels in epithelial cells from infected BALB/c mice but not in epithelial cells from infected AKR mice. Thus, using whole gut tissue, where the epithelial cell represents just a fraction of the material, RT-PCR revealed a weak but clear band for intelectin in infected BALB/c mice (Fig. 4). Using purified epithelial cells, intelectin transcripts can also be seen in naïve BALB/c mice with a marked up-regulation of expression postinfection. Transcripts for intelectin can also be seen in epithelial cells from naïve AKR mice. However, in AKR mice, there is a clear and profound down-regulation of expression of the intelectin gene in epithelial cells postinfection. Thus, importantly, the trend in the changes of intelectin gene expression is the same whether the analyses are conducted on whole gut tissue or epithelial cells: BALB/c mice up-regulate expression of intelectin postinfection, while AKR mice do not.

The time course of goblet cell hyperplasia correlates with worm expulsion and intelectin expression. The intestinal epithelium consists of enterocytes, enteroendocrine cells, Paneth cells, and goblet cells. Intelectin is considered within the literature as a predominantly Paneth-cell-derived molecule (28), with Paneth cells residing at the base of crypts of the small intestine. Although no Paneth cells are thought to exist in the large intestine, at least under resting uninfected conditions, there are sporadic reports of Paneth cells occurring within the colon in inflammatory conditions (26). However, using tissue from a separate infection experiment, histological staining for Paneth cells in gut sections from AKR and BALB/c mice at day 22 and day 34 postinfection failed to reveal any Paneth cells at the base of the large intestinal crypts, while *Trichinella spiralis*-infected small intestinal tissue, used as a positive control, was rich in Paneth cells (data not shown). Goblet cells are also rich sources of intelectin (39), and thus, groups of AKR and BALB/c mice were infected to examine the time course of goblet cell hyperplasia postinfection in these mouse strains. Although only correlative, Fig. 7 shows the presence of significantly more goblet cells in the gut tissue of BALB/c mice by day 22 postinfection ($P < 0.05$) than in the gut tissue of AKR mice. No increase from naïve levels in goblet cells is observed in AKR mice at this time point.

DISCUSSION

The polarization of lymph node cells towards Th1- or Th2-like phenotypes postinfection is well documented in the literature for a variety of parasites and is based primarily on cytokine secretion profiles from mesenteric lymph node cells (11, 13, 20). The intestinal nematode parasite *Trichuris muris* in the mouse is a model system which exemplifies polarized lymph node responses. Thus, a Th2 response (interleukin-4 [IL-4],

IL-5, IL-9, and IL-13) as seen in BALB/c mice underlies the host's ability to expel the parasite, and a Th1 response (IFN-γ) as seen in AKR mice results in chronic infection (4, 11, 13, 17, 20, 23). Less attention has been paid to the responses that occur locally in gut tissue in mouse strains resistant or susceptible to this helminth. We report here the first study to analyze the broad transcriptional responses of gut tissue during acute and chronic helminth infection. The data reveal that at the level of the gut, a mouse that is ultimately susceptible to infection responds very differently to the insult of infection with respect to its gene expression profile compared to that of a mouse that is able to expel the parasite.

BALB/c mice, which expelled the parasite by day 19 postinfection, responded to infection by up-regulating the expression of a variety of genes encoding potential antiparasitic proteins, namely intelectin, angiogenin-like protein, and angiogenin-related protein (24, 39, 43). Susceptible AKR mice showed an up-regulation of the gene coding angiogenin-like protein by day 60. However, expression levels of the other two genes were low at both day 19 and day 60. The intestinal epithelial cell forms the host-parasite interface and represents the niche within which *Trichuris* parasites burrow (37). We present data showing that epithelial cells from BALB/c mice represent one cellular source of intelectin within the gut. Within the epithelial cell compartment, Paneth cells and goblet cells are known sources of intelectin (28, 39). In the absence of any Paneth cells in the large intestine post-*Trichuris* infection, it is likely that the goblet cell (36, 39) is the cellular source of this antimicrobial activity, and indeed, goblet cell hyperplasia correlated with the kinetics of worm expulsion. Thus, BALB/c mice developed elevated numbers of goblet cells by day 22 postinfection. In AKR mice, no increase in goblet cell numbers from uninfected levels was seen until day 34, when numbers were starting to rise. However, by this time, adult parasites which are less readily expelled had developed. Thus, early stages of *T. muris* are immunogenic and can be expelled by appropriate (but as-yet-undefined) effector mechanisms. Later, larval stages modulate immunity to promote their own survival, and potential effector mechanisms become less effective (12). Hence, the rate at which an effector response develops in relation to the parasite growth rate is at least as, if not more, important as the level of that response.

Thus, our data suggest that one component of the host protective immune response to *Trichuris* may involve the local release of innate antimicrobial factors such as intelectin by cells within the gut. Supporting this, it has recently been suggested that goblet cell-derived intelectin, in this case intelectin 2, may play an important role in the innate immune response to *Trichinella spiralis* (39). Since the recent description of mouse intelectin 2 in the literature (38), and using the differential PCR for intelectin 1 and intelectin 2 described previously (39), we have extended our own data to show that BALB/c mice infected with *T. muris* express both intelectin 1 and intelectin 2 (R. Datta and K. J. Else, unpublished data). Precisely how these factors might be involved in worm expulsion is not clear, although they may recognize carbohydrates on the surface of nematodes (43). At the time points analyzed, we did not detect a significant up-regulation of genes encoding Th2 cytokines in gut tissue from resistant mice, although goblet cell hyperplasia, which proceeds more potently in the resistant strain, is under the control of Th2 cytokines (25). The detection of changes in typical Th2-associated transcripts may require analyses to be performed on gut tissue taken at earlier time points or the purification of T cells from gut tissue for gene expression profiling.

The much-documented Th1 response that dominates the mesenteric lymph node of susceptible mice (4, 9, 13, 17, 20, 23) is also reflected in the gene expression profiles of gut tissue, with the expression of a variety of IFN-γ-regulated genes increasing at day 19 postinfection. These include the chemokines CXCL11 and CXCL9 and T-cell-specific GTPase. Surprisingly, by microarray, we did not see a significant increase in expression of the IFN-γ gene itself. However, RT-PCR analyses showed the presence of IFN-γ transcripts in gut tissue taken from infected AKR mice at this time postinfection (Fig. 5), and thus, our inability to detect any up-regulation by microarray may simply reflect a difference in the sensitivity of the two assays when whole gut tissue is used. Certainly, microarray analyses of mesenteric lymph node responses in AKR mice revealed a significant increase ($\log_2$ 1.3) in the transcripts for IFN-γ at day 19 postinfection (data not shown). The data presented in this paper are based on the use of glass oligonucleotide arrays. Through their use, it emerged that despite providing strong, robust data for up-regulated, abundant transcripts, they did lack sensitivity for low-abundance transcripts. Thus, to further evaluate the key candidate genes highlighted by their prominence on the glass arrays, a third biological repeat (i.e., a new infection) in AKR and BALB/c mice was performed, and the gene expression profiles were analyzed at day 19 postinfection using a completely different microarray platform, the Affymetrix chip. The results of this confirmed the original analyses, and in all cases, genes represented on both arrays and which form the core of the paper followed entirely similar patterns. Thus, by Affymetrix, expression of the genes for intelectin, mouse mast cell protease 1, pancreatic lipase-related protein 2, chloride channel calcium-activated 3, and somatostatin were more highly up-regulated from uninfected levels in resistant BALB/c gut tissue than in AKR gut tissue, as also seen in Fig. 1. As before, of these genes, only mouse mast cell protease 1 was also elevated in the AKR host. Thus, the $\log_2$-fold changes for these genes were as follows: intelectin, 6.5 for BALB/c and −0.6 for AKR mice; mouse mast cell protease 1, 6.0 for BALB/c and 2.5 for AKR mice; pancreatic lipase-related protein 2, 5.0 for BALB/c and 0.1 for AKR mice; chloride channel calcium-activated 3, 1.8 for BALB/c and −0.7 for AKR mice; and somatostatin, 1.4 for BALB/c and −0.1 for AKR mice. Figure 1 also shows the genes which were more highly up-regulated from uninfected levels in susceptible AKR gut tissue than in the BALB/c host. These changes were also mirrored on the Affymetrix chip, with $\log_2$-fold increases in expression postinfection relative to naïve levels of indoleamine-2,3-dioxygenase of 6.5 for AKR and −0.04 for BALB/c mice; pancreatitis-associated protein of 1.9 for AKR and −1.7 for BALB/c mice; CXCL11 of 4.8 for AKR and 0.0 for BALB/c mice; tryptophan tRNA synthase of 3.9 for AKR and 0.14 for BALB/c mice; T-cell-specific GTPase of 5.3 for AKR and 0.7 for BALB/c mice; Z-DNA binding protein 1 of 1.3 for AKR and −0.3 for BALB/c mice; Ia-associated invariant chain of 4.2 for AKR and 1.8 for BALB/c mice; and CXCL9 of 5.4 for AKR and −0.2 for BALB/c mice. Interestingly, in susceptible mice,

we identified two IFN-γ-induced genes which are part of the tryptophan metabolism pathway: indoleamine-2,3-dioxygenase (Indo) and tryptophan tRNA synthetase (Wars). Wars is thought to be induced in cells to allow their survival in low-tryptophan concentrations. Indoleamine-2,3-dioxygenase is the rate-limiting enzyme in the metabolism of tryptophan through the kynurenine pathway. Indoleamine-2,3-dioxygenase is known to be up-regulated in tissue infected with a variety of parasites, but its function in these instances is thought to be in the depletion of tryptophan and thus inhibition of parasite growth (19, 22, 42). Its presence here in susceptible mice where the worms are thriving, and absence from resistant mice, suggests a more interesting role relating to the recent literature on the role of indoleamine-2,3-dioxygenase in immunoregulation and T-cell suppression demonstrated in vitro and in vivo (15, 30–32, 35). Thus, its dominance in local tissues of chronically infected mice may represent a survival strategy of the parasite either by suppressing the functions of effector T cells or by dampening down potentially damaging host inflammation. Its induction by IFN-γ and the knowledge that *T. muris* expresses an IFN-γ-like homologue (21) make this hypothesis even more attractive. Coinduction of the transcripts for indoleamine-2,3-dioxygenase and Wars has previously been demonstrated in a proteomic analysis of the proteins present in the mucosa of humans with inflammatory bowel disease and a T-cell-regulatory role proposed previously (5). As far as we are aware, their coinduction has not been described before for intestinal nematode parasites in the context of resistance and susceptibility to infection.

In addition to genes with up-regulated expression postinfection, we identified genes with down-regulated expression postinfection. Interestingly, at day 19 postinfection, there were almost three times as many genes down-regulated in expression in susceptible AKR mice compared to that in resistant BALB/c mice. Although the significance of this is not clear as yet, it is possible that the absence of gene expression products rather than their presence is contributing to the failure to clear the parasite. Equally, some of these down-regulated genes may simply be markers of persisting infection. For instance, the expression of carbonic anhydrase (Car2) is reduced in gut tissue of AKR mice at both day 19 and day 60 postinfection and has also been shown to be reduced postinfection in other models of intestinal parasite infections (1). Equally, the decrease in transcripts for the water channel aquaporin 8 may be a response by the host to decrease fluid transport across the epithelium during chronic infection. Indeed, cholera toxin has been shown to induce similar changes in the intestinal mucosa of rats (18). Here, the down-regulation of transcripts for aquaporin 8 was suggested to play a role in diminishing water transport during cholera.

Microarray analyses have been used to characterize the gene expression profiles of a variety of infections and diseases of the intestine including inflammatory bowel disease (10) and *Helicobacter* infection (33, 34). Using microarray, Sandler et al. (40) have recently described distinct gene expression profiles of Th1- and Th2-type granulomas. Here, transcripts up-regulated in Th1-type granulomas were associated with tissue damage, while the gene expression profiles of Th2 granulomas were more related to fibrosis and wound healing. Our study also reveals distinct gene expression profiles in a Th1/Th2-dominated model but for the first time also places the gut tissue responses in the context of resistance and susceptibility to the pathogen, highlighting candidate genes which may play roles in both worm elimination and worm survival.

ACKNOWLEDGMENTS

This work was supported by the BBSRC (34/S15449) and the Wellcome Trust (044494 and 068639).

We acknowledge the MRC Rosalind Franklin Centre for Genomics Research (formally the UK Human Genome Mapping Project Resource Centre) for support and supply of the microarrays and Andy Hayes for use of the microarray facility at Manchester. We also thank G. Anderson for the G8.8 monoclonal antibody.

REFERENCES

1. **Aleksandersen, M., L. Kai-Inge, B. Gjerde, and T. Landsverk.** 2002. Lymphocyte depletion in ileal Peyer's patch follicles in lambs infected with *Eimeria ovinoidalis*. Clin. Diagn. Lab. Immunnol. **9:**83–91.
2. **Artis, D., N. E. Humphreys, C. S. Potten, N. Wagner, W. Müller, J. R. McDermott, R. K. Grencis, and K. J. Else.** 2000. β7 integrin-deficient mice: delayed leukocyte recruitment and attenuated protective immunity in the small intestine during enteric helminth infection. Eur. J. Immunol. **30:**1656–1664.
3. **Artis, D., C. S. Potten, K. J. Else, F. D. Finkelman, and R. K. Grencis.** 1999. *Trichuris muris*: host intestinal epithelial cell hyperproliferation during chronic infection is regulated by interferon-γ. Exp. Parasitol. **92:**144–153.
4. **Bancroft, A. J., A. N. J. McKenzie, and R. K. Grencis.** 1998. A critical role for IL-13 in resistance to intestinal nematode infection. J. Immunol. **160:**3453–3461.
5. **Barceló-Batllori. S., M. André, C. Servis, N. Lévy, O. Takikawa, P. Michetti, M. Reymond, and E. Felley-Bosco.** 2002. Proteomic analysis of cytokine induced proteins in human intestinal epithelial cells: implications for inflammatory bowel diseases. Proteomics **2:**551–560.
6. **Betts, C. J., and K. J. Else.** 1999. Mast cells, eosinophils and antibody mediated cytotoxicity are not critical in resistance to *Trichuris muris*. Parasite Immunol. **21:**45–52.
7. **Betts, C. J., M. L. deSchoolmeester, and K. J. Else.** 2000. *Trichuris muris*: CD4+ T cell mediated protection in reconstituted SCID mice. Parasitology **121:**631–637.
8. **Cornell, M., N. W. Paton., C. Hedeler, P. Kirby, D. Delneri, A. Hayes, and S. G. Oliver.** 2003. GIMS: an integrated data storage and analysis environment for genomic and functional data. Yeast **20:**1291–1296.
9. **deSchoolmeester, M. L., M. C. Little, B. J. Rollins, and K. J. Else.** 2003. Absence of CC chemokine ligand 2 results in an altered Th1/Th2 cytokine balance and failure to expel *Trichuris muris* infection. J. Immunol. **170:**4693–4700.
10. **Dieckgraefe, B. K., W. F. Stenson, J. R. Korzenik, P. E. Swanson, and C. A. Harrington.** 2000. Analysis of mucosal gene expression in inflammatory bowel disease by parallel oligonucleotide arrays. Phys. Genom. **4:**1–11.
11. **Else, K. J., and F. D. Finkelman.** 1998. Intestinal nematode parasites, cytokines and effector mechanisms. Int. J. Parasitol. **28:**1145–1158.
12. **Else, K. J., D. Wakelin, and T. I. A. Roach.** 1989. Host predisposition to trichuriasis: the mouse-*T. muris* model. Parasitology **89:**275–282.
13. **Else, K. J., F. D. Finkelman, C. R. Maliszewski, and R. K. Grencis.** 1994. Cytokine-mediated regulation of chronic intestinal helminth infection. J. Exp. Med. **179:**347–351.
14. **Else, K. J., D. Wakelin, D. L. Wassom, and K. M. Hauda.** 1990. The influence of genes mapping within the major histocompatibility complex on resistance to *Trichuris muris* infections in mice. Parasitology **101:**61–67.
15. **Fallarino, F., U. Grohmann, K. W. Hwang, C. Orabona, C. Vacca, R. Bianchi, M. L. Belladonna, M. C. Fioretti, M. L. Alegre, and P. Puccetti.** 2003. Modulation of tryptophan catabolism by regulatory T cells. Nat. Immunol. **4:**1206–1212.
16. **Fang, Y., A. Brass, D. C. Hoyle, A. Hayes, A. Bashein, S. G. Oliver, D. Waddington, and M. Rattray.** 2003. A model-based analysis of microarray experimental error and normalisation. Nucleic Acids Res. **31:**e96.
17. **Faulkner, H., J.-C. Renauld, J. Van Snick, and R. K. Grencis.** 1998. Interleukin-9 enhances resistance to the intestinal nematode *Trichuris muris*. Infect. Immun. **66:**3832–3840.
18. **Flach, C.-F., S. Lange, E. Jennische, and I. Lonnroth.** 2004. Cholera toxin induces expression of ion channels and carriers in rat small intestinal mucosa. FEBS Lett. **561:**122–126.
19. **Fujigaki, S., K. Saito, M. Takemura, N. Maekawa, Y. Yamada, H. Wada, and M. Seishima.** 2002. L-Tryptophan–L-kynurenine pathway metabolism accelerated by *Toxoplasma gondii* infection is abolished in gamma interferon-gene-deficient mice: cross-regulation between inducible nitric oxide synthase and indoleamine-2,3-dioxygenase. Infect. Immun. **70:**779–786.
20. **Grencis, R. K.** 2001. Cytokine regulation of resistance and susceptibility to

intestinal nematode infection—from host to parasite. Vet. Parasitol. **100:**45–50.
21. **Grencis, R. K., and G. M. Entwistle.** 1997. Production of an interferon-gamma homologue by an intestinal nematode: functionally significant or interesting artefact? Parasitology **115:**S101–S106.
22. **Grohmann, U., F. Fallarino, and P. Puccetti.** 2003. Tolerance, DCs and tryptophan: much ado about IDO. Trends Immunol. **24:**242–248.
23. **Helmby, H., K. Taleda, S. Akira, and R. K. Grencis.** 2001. Interleukin (IL)-18 promotes the development of chronic gastrointestinal helminth infection by down regulating IL-13. J. Exp. Med. **194:**355–364.
24. **Hooper, L. V., T. S. Stappenbeck, C. V. Hond, and J. I. Gordon.** 2003. Angiogenins: a new class of microbicidal proteins involved in innate immunity. Nat. Immunol. **4:**269–273.
25. **Ishikawa, N., D. Wakelin, and Y. R. Mahida.** 1997. Role of T helper 2 cells in intestinal goblet cell hyperplasia in mice infected with *Trichinella spiralis*. Gastroenterology **113:**542–549.
26. **Kelly, P., R. Feakins, P. Domizio, J. Murphy, C. Bevins, J. Wilson, G. McPhail, R. Poulsom, and W. Dhaliwal.** 2004. Paneth cell granule depletion in the human small intestine under infective and nutritional stress. Clin. Exp. Immunol. **135:**303–309.
27. **Knight, P. A., S. H. Wright, J. K. brown, X. Huang, D. Sheppard, and H. R. P. Miller.** 2002. Enteric expression of the integrin αvβ6 is essential for nematode-induced mucosal mast cell hyperplasia and expression of the granule chymase, mouse mast cell protease 1. Am. J. Pathol. **161:**771–779.
28. **Komiya, T., Y. Tanigawa, and S. Hirohashi.** 1998. Cloning of the novel gene intelectin, which is expressed in intestinal paneth cells in mice. Biochem. Biophys. Res. Commun. **251:**759–762.
29. **McDermott, J. R., R. E. Bartram, P. A. Knight, H. R. P. Miller, D. R. Garrod, and R. K. Grencis.** 2003. Mast cells disrupt epithelial barrier function during enteric nematode infection. Proc. Natl. Acad. Sci. USA **100:**7761–7766.
30. **Mellor, A. L., B. Baban, P. Chandler, B. Marshall, K. Jhaver, A. Hansen, P. A. Koni, M. Iwashima, and D. H. Munn.** 2003. Cutting edge: induced indoleamine 2,3 dioxygenase expression in dendritic cell subsets suppresses T cell clonal expansion. J. Immunol. **171:**1652–1655.
31. **Mellor, A. L., and D. H. Munn.** 1999. Tryptophan catabolism and T-cell tolerance: immunosuppression by starvation? Immunol. Today **20:**469–473.
32. **Mellor, A. L., and D. H. Munn.** 2003. Tryptophan catabolism and regulation of adaptive immunity. J. Immunol. **170:**5809–5813.
33. **Mueller, A., J. O'Rourke, P. Chu, C. C. Kim, P. Sutton, A. Lee, and S. Falkow.** 2003. Protective immunity against *Helicobacter* is characterized by a unique transcriptional signature. Proc. Natl. Acad. Sci. USA **100:**12289–12294.
34. **Mueller, A., J. O'Rourke, J. Grimm, K. Guillemin, M. F. Dixon, A. Lee, and S. Falkow.** 2003. Distinct gene expression profiles characterize the histopathological stages of disease in *Helicobacter*-induced mucosa-associated lymphoid tissue lymphoma. Proc. Natl. Acad. Sci. USA **100:**1292–1297.
35. **Munn, D. H., E. Shaftzadeh, J. T. Attwood, I. Bondariec, A. Pashine, and A. L. Mellor.** 1999. Inhibition of T cell proliferation by macrophage tryptophan catabolism. J. Exp. Med. **189:**1363–1372.
36. **Ouellette, A. J.** 1999. IV. Paneth cell antimicrobial peptides and the biology of the mucosal barrier. Am. J. Physiol. **277:**G257–G261.
37. **Panesar, T. S.** 1981. The early phase of tissue invasion by *Trichuris muris* (Nematoda: Trichuroidea). Zetschrifte Parasitenkunde **66:**163–166.
38. **Pemberton, A. D., P. A. Knight, S. H. Wright, and H. R. P. Miller.** 2004. Proteomic analysis of mouse jejunal epithelium and its response to infection with the intestinal nematode, *Trichinella spiralis*. Proteomics **4:**1101–1108.
39. **Pemberton, A. D., P. A. Knight, J. Gamble, W. H. Colledge, J.-K. Lee, M. Pierce, and H. R. P. Miller.** 2004. Innate BALB/c enteric epithelial response to *Trichinella spiralis*: inducible expression of a novel goblet cell lectin, intelectin-2, and it natural deletion in C57BL/10 mice. J. Immunol. **173:**1894–1901.
40. **Sandler, N. G., M. M. Mentink-Kane, A. W. Cheever, and T. A. Wynn.** 2003. Global gene expression profiles during acute pathogen-induced pulmonary inflammation reveal divergent roles for Th1 and Th2 responses in tissue repair. J. Immunol. **171:**3655–3667.
41. **Schopf, L. R., K. F. Hoffmann, A. W. Cheever, J. F. Urban, Jr., and T. A. Wynn.** 2002. IL-10 is critical for host resistance and survival during gastrointestinal helminth infection. J. Immunol. **168:**2383–2392.
42. **Silva, N. M., C. V. Rodrigues, M. M. Santoro, L. F. L. Reis, J. I. Alvarez-Leite, and R. T. Gazzinelli.** 2002. Expression of indoleamine 2,3-dioxygenase, tryptophan degradation, and kynurenine formation during in vivo infection with *Toxoplasma gondii*: induction by endogenous gamma interferon and requirement of interferon regulatory factor 1. Infect. Immun. **70:**859–868.
43. **Tsuji. S., J. Yehori, M. Matsumoto, Y. Suzuki, A. Matsuhisa, K. Toyoshima, and T. Seya.** 2001. Human intelectin is a novel soluble lectin that recognizes galactofuranose in carbohydrate chains of bacterial cell wall. J. Biol. Chem. **276:**23456–23463.
44. **Tusher, V. G., R. Tibshirani, and G. Chu.** 2001. Significance analysis of microarrays applied to the ionizing radiation response. Proc. Natl. Acad. Sci. USA **98:**5116–5121.

Editor: J. F. Urban, Jr.